

Construction of the Scanning Transmission X-ray Microscope Beamline at UVSOR

This content has been downloaded from IOPscience. Please scroll down to see the full text.

2013 J. Phys.: Conf. Ser. 463 012006

(<http://iopscience.iop.org/1742-6596/463/1/012006>)

View [the table of contents for this issue](#), or go to the [journal homepage](#) for more

Download details:

IP Address: 133.48.171.224

This content was downloaded on 21/11/2013 at 04:54

Please note that [terms and conditions apply](#).

Construction of the Scanning Transmission X-ray Microscope Beamline at UVSOR

T Ohigashi¹, H Arai¹, T Araki², N Kondo¹, E Shigemasa¹, A Ito^{1,3}, N Kosugi¹ and M Katoh¹

¹Institute for Molecular Science, 38 Nishigo-naka, Myodaiji, Okazaki, Aichi 444-8585, Japan

²TOYOTA Central R&D Labs., Inc., 41-1, Yokomichi, Nagakute, Aichi 480-1192, Japan

³Tokai University, 4-1-1 Kitakaname, Hiratsuka, Kanagawa 259-1292, Japan

E-mail: ohigashi@ims.ac.jp

Abstract. Construction of a scanning transmission x-ray microscope (STXM) beamline is in progress at UVSOR (Okazaki, Japan). To obtain high brilliance with high resolving power for the incident x-rays, the combination of an in-vacuum undulator and a Monk-Gillieson mounting monochromator with a varied line spacing plane grating was adopted. Resolving power, spectrum and size of the incident x-rays of the beamline were discussed through simulations. Then the photon flux at a sample of $\sim 10^8$ photons/s at the resolving power of 5,000 in the photon energy range from 100 to 700 eV is expected. As the first results, spectrum of calcium in chalk is shown.

1. Introduction

The scanning transmission x-ray microscopy (STXM) is a powerful tool to perform 2-dimensional mapping of the x-ray spectroscopy with spatial resolution of several tens of nm. This method is appropriate for using the soft x-ray region covering the K absorption edges of light elements and the L absorption edges of transition metals. These absorption edges make the STXM useful for study of functional materials, such as polymers and carbon nanotubes. In addition, using the energy range between the K absorption edges of carbon and oxygen (282~539 eV), called the “water window” region, enables us to observe samples in water, such as cells, with high spatial resolution. For these features, the STXM used in the soft x-ray region becomes a unique technique in broad research fields. To achieve a satisfactory performance of the STXM, a tunable x-ray source with high brilliance, such as a synchrotron radiation, is necessary. In these years, several STXM systems have been installed at synchrotron radiation facilities, Advanced Light Source [1, 2], Swiss Light Source [3], BESSY [4], Canadian Light Source [5], National Synchrotron Light Source [6], Shanghai Light Source Facility [7], Elettra [8] and more to come. The UVSOR facility (Okazaki, Japan), is a synchrotron light source (750 MeV, 300 mA) designed for using the photon energy from IR to soft x-rays. In 2012, the storage ring of the UVSOR-II was upgraded to UVSOR-III to increase the brilliance by reducing the



emittance from 27 to 15 nmrad. In the upgrade project, an in-vacuum undulator was also installed at the short straight section for the new STXM beamline, BL4U. These improvements and energy specification of the facility are suitable to operate the STXM with a satisfactory performance so that the construction project of the new STXM beamline, BL4U, has been launched.

In this report, the concept of the STXM beamline project, its current status and the perspectives are shown.

2. Construction of the beamline

To achieve a satisfactory performance of the STXM, it is important to use the incident x-rays with high brilliance and stability. In our beamline, the in-vacuum undulator is used as an x-ray source. The undulator has 26 magnetic periods with the period length of 38 mm pitch and the gap width can be changed from 13 to 40 mm. Brightness of the x-ray source with the undulator, calculated by using SPECTRA [9], was plotted in Fig. 1 against the energy with changing the gap width. These plots show that the photon energy range from 100 to 700 eV can be used effectively.

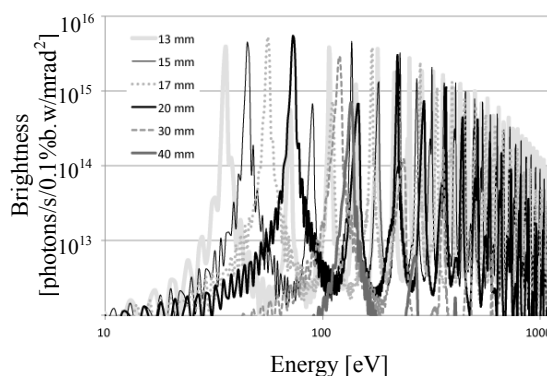


Fig. 1: Calculated brightness of the x-ray source with the in-vacuum undulator with changing the gap

2.1. Monochromator

Our beamline employed a variable-included-angle Monk-Gillieson mounting monochromator with a varied line spacing plane grating (VLSPG) [10]. The monochromator consists of 3 mirrors, grating and two slits. A schematic image of the optical system is shown in Fig. 2. The incident x-rays from the undulator enters a toroidal mirror M_0 ($R=3725.09$ m and $\rho=0.2193$ m), which is set 6.5 m downstream from the light source with the incident angle of 88° through a slit, S_1 . The M_0 mirror focuses the incident x-rays onto a fixed exit slit, S_2 , downstream 6.29 m vertically and collimates the x-ray horizontally. The collimated beam is reflected vertically by a plane mirror, M_1 , and enters the VLSPG. The line spacing of the VLSPG, N , is given by $N=N_0 \cdot (1+a_1 \cdot x+a_2 \cdot x^2+a_3 \cdot x^3)$, where x is a position on the VLSPG and its parameters as follows; $N_0=500$ lines/mm, $a_1=-3.9534 \times 10^{-4}$ mm $^{-1}$, $a_2=1.1668 \times 10^{-7}$ mm $^{-2}$ and $a_3=-3.1044 \times 10^{-11}$ mm $^{-3}$. Sum of the incident angles of the M_1 and the VLSPG varies from 167 to 176° . The beam is focused onto the S_2 horizontally by a cylindrical mirror, M_2 ($R=85.963$ m) with the incident angle of 88° . Ray-trace simulations of shapes of the beams at the S_2 with changing the resolving power, $E/\Delta E$, of 3,000, 5,000, 10,000 and 20,000 with their vertical FWHMs are shown in Fig. 3. The main photon energy was fixed at 285 eV. These ray-tracing simulations were performed by X.O.P [11]. From Fig. 3, the FWHMs of the vertical beam size (*i.e.* required width of the S_2) become smaller with increasing the $E/\Delta E$ and converge at around that of 22 μm . Therefore, the $E/\Delta E$ of 10,000~ is considered as the maximum resolving power of our beamline from Fig. 3(c) and 3(d). Practically, it is effective for performance of

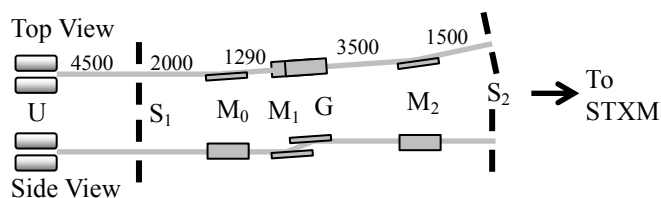


Fig. 2: Schematic images of the optical system of BL4U, where U: the in-vacuum undulator, S_1 : the slit, M_0 : the toroidal mirror, M_1 : the plane mirror, G: the varied line spacing plane grating, M_2 : the cylindrical mirror and S_2 : the fixed exit slit. The unit of the length is mm.

the STXM to use more photon flux rather than the higher $E/\Delta E$ than 5,000 (*i.e.* width of the S_2 is set as $30\ \mu\text{m}$).

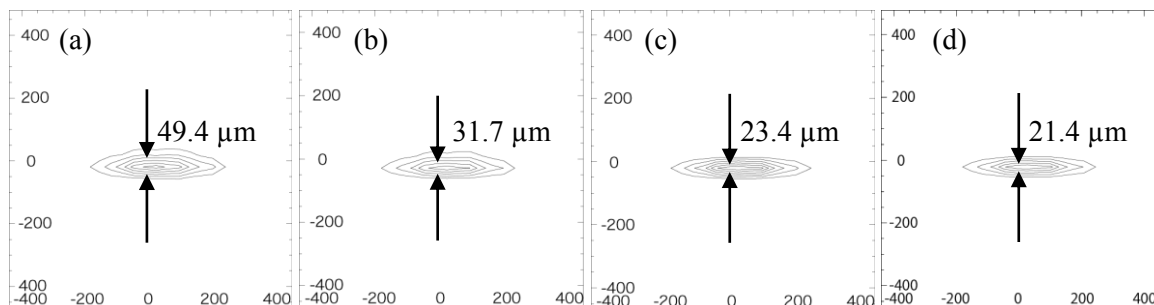


Fig. 3: Ray-trace simulations of the shapes of the monochromatized beams at the fixed exit slit at the $E/\Delta E$ of (a) 3,000, (b) 5,000, (c) 10,000 and (d) 20,000 with their vertical FWHMs. The main photon energies are 285 eV. The unit of length is μm .

2.2. Scanning transmission x-ray microscope

A Fresnel Zone Plate (FZP) is used as a focusing optical device. By using the S_2 as a virtual source, the FZP placed at 1,334 mm downstream from the S_2 focuses the x-rays onto the sample through an order sorting aperture. With raster scanning of the sample by piezo stages, the transmitted x-rays are detected by a photon multiplier tube with scintillator.

We have been preparing two FZPs, whose parameters are the outermost width of 25 nm, the diameter of 240 μm , the number of the zones of 2,400 and the pattern material of gold or nickel of 100 nm thick. Calculated efficiencies of the FZPs made of gold and nickel, including transmittance of Si_3N_4 support membrane of 100 nm thick, are plotted in Fig. 4. In these plots, the efficiency of the nickel FZP is better than the energy region from 170 to 504 eV so that using the nickel one is more effective to analyze the elements in this region, such as carbon and nitrogen. Totally, by taking into account of efficiency of the FZP, the photon flux of $\sim 10^8$ photons/sec at the sample at $E/\Delta E=10,000$ is expected for our beamline.

To obtain the diffraction-limited spatial resolution for the STXM, the expected focusing spot size of ~ 30 nm, the FZP should be illuminated by the incident x-rays with longer coherent length than its diameter and with the $E/\Delta E$ bigger than number of the zones of the FZP, 2,400. The radius of the coherent area R with coherency of 0.88 is given by $R=0.32z\lambda/D$, where z is the distance between the source and the FZP, λ is the wavelength of the incident x-ray and D is size of aperture of the fixed exit slit, S_2 . For the coherent illumination at C K-edge (285 eV), D should be set as 15.5 μm while the $E/\Delta E$ becomes more than 10,000. Then, a simulated shape of the incident beam at the FZP is shown in Fig. 5. This beam size of 1.5 (H) \times 1.9 (V) mm^2 is large enough to illuminate whole FZP, 240 μm . Therefore, the diffraction-limited spatial resolution is available in this condition.

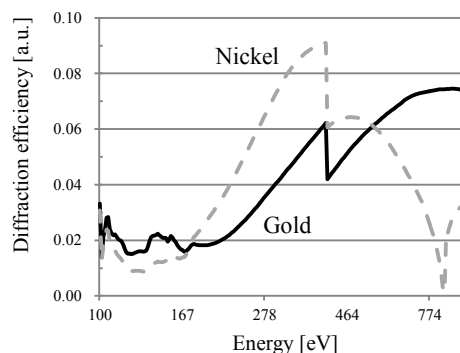


Fig. 4: Calculated efficiencies of the FZPs made of gold and nickel including transmittance of Si_3N_4 substrate membrane

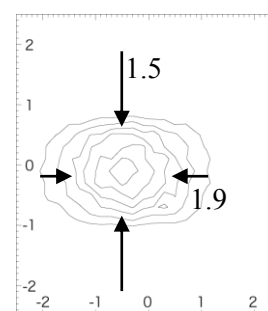


Fig. 5: Simulated shape of the incident beam at the FZP for the diffraction-limited spatial resolution. The unit of length is mm.

However, the photon flux is estimated to be about one order less than the condition of S_2 for $E/\Delta E = 10,000$.

3. Commissioning of the beamline

In late September 2012, the construction of the beamline was finished and its alignment is started in October. The monochromator is calibrated by measuring K absorption edge spectrum of nitrogen gas (shown in Fig. 6) with setting the S_2 as 30 μm width. From ratio of heights of π^* peak and valley, the $E/\Delta E$ was estimated as around 6,000 and this result was reasonable compared with Fig. 3 (b). From December, the STXM is commissioned and grinded particles of a chalk on microgrid were observed as the first sample by noticing L absorption edge of calcium. 91 Transmitted x-ray images were acquired every 0.1 eV from 346 to 356 eV and the image at 346 eV is shown in Fig. 7 (a) as an example. From area in Fig 7 (a) indicated by a dotted circle, spectrum of optical density of calcium of the chalk is obtained and is shown in Fig. 7 (b). Four peaks, which are assumed to be calcium oxide, are clearly seen on the plot.

We have been improving our beamline for using wider energy region, stability and calibrations. Our beamline is due to open for general users in June 2013.

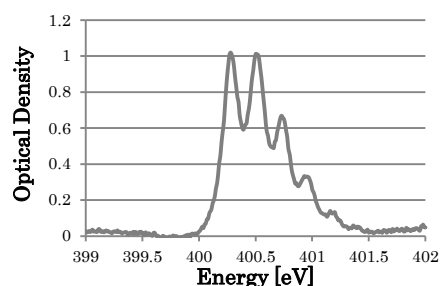


Fig. 6: Spectrum of nitrogen gas

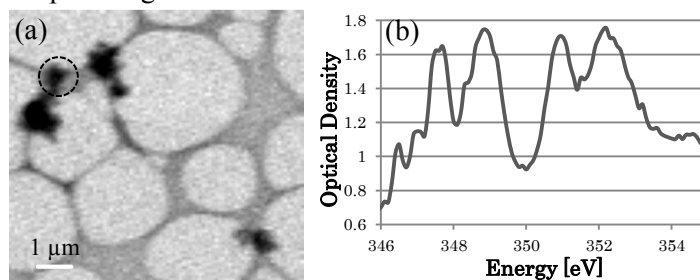


Fig. 7: STXM observation of chalk particles on microgrid (a) transmission image at 346 eV and (b) spectrum of the chalk indicated by a dotted circle in (a)

References

- [1] Kilcoyne A L D *et al* 2003 *J. Synchrotron Rad.* **10** 125-136
- [2] Bluhm H *et al* 2006 *J. Electron Spectrosc. Relat. Phenom.* **150** 86-104
- [3] Raabe J *et al* 2008 *Rev. Sci. Instrum.* **79** 113704
- [4] Wiesemann U *et al* 2003 *J. Phys. IV France* **104** 95-98
- [5] Kaznatcheev K V *et al* 2007 *Nucl. Instr. Meth. Phys. Res. A* **582** 96-99
- [6] Kirz J *et al* 1992 *Rev. Sci. Instrum.* **63** 557-563
- [7] Xue C *et al* 2010 *Rev. Sci. Instrum.* **81** 113502
- [8] Kaulich B *et al* 2006 *IPAP Conf. Series* **7** pp 22-25
- [9] <http://radiant.harima.riken.go.jp/spectra/index.html>
- [10] Koike M and Namioka T 1995 *Rev. Sci. Instrum.* **66** 049501
- [11] <http://www.esrf.eu/computing/scientific/xop2.1/>